Experimental evaluation of heat transfer coefficient for nanofluids

Carla MENALE [1,*], Francesco D'ANNIBALE [2], Andrea MARIANI [2], Roberto BUBBICO [1]

* Corresponding author: Tel.:++39 0630486467; Email: carla.menale@enea.it
1 DICMA, "Sapienza" University of Rome, Rome, Italy
2 ENEA Laboratory of Thermal Fluid Dynamics, Rome, Italy

Abstract The paper reports the results of heat transfer experimental tests on nanofluids. Measurements were performed in a two-loop test rig for immediate comparison of the thermal performances of the nanofluid with the base-fluid. The convective heat transfer was evaluated in a circular pipe heated with uniform heat flux and with flow regimes from laminar to turbulent. Tests have been performed to compare the heat transfer capability of nanofluids and water at the same velocity or Reynolds number, and they have been compared with values calculated from widely used correlations. In particular ten different nanofluids and three base fluids (in addition to the water) have been used.
The analysis of the experimental data shows a different behavior depending on the parameter used in the comparison, and, as a consequence, the addition of nanoparticles to the heat transfer fluid can result advantageous or not, depending on the specific point of view. Furthermore some classical correlations have been used to estimate the heat transfer coefficients, and the analysis shows that they are able to provide good agreement with the experimental data both for the nanofluid and water.

Keywords: Nanofluids, Heat transfer, Base fluid, Laminar, Turbulent

1. Introduction

In recent years the international research community has shown significant interest in investigating nanofluids, and several review papers are available in this field [1-6]. Nanofluids are a new class of coolants engineered by dispersing and stably suspending in base fluids a limited amount of nanoparticles (metallic or non-metallic) with typical size on the order of 1-100 nm, and expected to offer important advantages over conventional heat transfer fluids and with limited mechanical effects compared to larger particles suspensions [2,3, 6-9].

Numerous models have been proposed to account for this unexpected thermal behavior, but uncertainties in the reported experimental values and controversies in the proposed mechanisms still remain [1-5], and papers about thermal enhancement sometimes report also the presence of sparse and inconsistent and/or contradictory experimental results from different laboratories [4,5]. At the same time several other works reported convective heat transfer properties similar to the values calculated by traditional models ([4], [10-12]),

showing the behavior of a homogeneous mixture without any abnormal increase.

One of the main problems is the scarce agreement of the results obtained by different researchers in the determination of heat transfer coefficients. In order to solve this problem a specifically dedicated facility was designed as two identical loops working simultaneously under the same experimental conditions, one loop being filled with the nanofluid and the other with the base fluid. One of the main uncertainties of the available experimental results is in fact related to the determination modality of the heat transfer enhancement: usually by comparing the measured heat transfer coefficient of the nanofluid either with the equivalent data obtained at different times with the base fluid, or with the value for the pure fluid calculated with traditional correlations under the same operating conditions. This procedure can introduce possible errors in the results, because, in the first case, it is very difficult to reach identical conditions at different times, while in the second case the correlation uncertainty can be comparable with the measured difference.

In the present paper we will report the results obtained in the determination of the heat transfer rate for ten different nanofluids, and the comparison with pure water or other base fluids like water-ethylene glycol solution.

2. Nanofluids

The tested nanofluids are reported in Table 1. They are made of nanoparticles suspended in a base fluid (water or water/ethylene glycol solutions) added with a small amount of surfactant necessary to limit agglomeration. The nanoparticle materials are TiO_2, ZrO_2, SiC and Al_2O_3, dispersed in different concentrations (3wt% to 20wt%).

The uncertainties of the physical properties are 2% for the thermal conductivity, 4% for the viscosity. The specific heat is calculated from the model based on the heat capacity of each phase, with an accuracy of about 2%:

$$c_{p,N} = \frac{(1-\phi_{vol})(\rho c_p)_{BF} + \phi_{vol}(\rho c_p)_P}{\rho_N} \quad (1)$$

The density is measured directly by a Coriolis flow meter during the test with an accuracy higher than 0.7%. The resulting maximum uncertainty of the calculated heat transfer coefficient is 8%.

Table 1
Nanofluid characteristics (viscosity and density are referred to water)

nanofluid	weight fraction	volume fraction	base fluid/surface modifier	viscosity ratio	density ratio	particle size [nm]
TiO_2	9%	2.3%	H_2O/PC	1.88	1.099	20-30
TiO_2	9%	2.3%	H_2O/PA	1.16	1.095	15
ZrO_2	9%	1.7%	H_2O/ PA	1.972	1.084	100
b.f.-ZrO_2	0%	0%	H_2O/ PA	8.50	1.0047	
SiC	9%	3.0%	H_2O/ PA	1.32	1.047	25
SiC	6%	2.0%	H_2O/ PA	1.32	1.027	25
SiC	3%	1.0%	H_2O/ PA	1.32	1.01	25
Al_2O_3	9%	2.4%	H_2O/OS	1.475	1.076	100-200
Al_2O_3	3%	0.8%	H_2O/ OS	1.124	1.036	100-200
Al_2O_3	9%	2.4%	H_2O/ OS + CA		1.076	100-200
Al_2O_3	9%	2.4%	H_2O/ OS + MA		1.076	100-200
Al_2O_3	9%	2.4%	H_2O-AF 50-50/?	4.3	1.146	150
b.f. Al_2O_3	0%	0%	H_2O-AF 50-50/?	3.2	1.066	
Al_2O_3	20%	5.33%	H_2O-EG 50-50/OS	6.3	1.259	100
b.f. Al_2O_3	0%	0%	H_2O-EG 50-50/OS	3.1	1.057	

PC=Polycarboxylate; PA=Polyacrilate; OS=Octylsilane; AF=Antifrogen_N; EG=ethylene glycol; CA=citric acid; MA= malic acid; ?= unknown

3. The Hetna Test Rig

The HETNA (Hydraulic Experiments on Thermo-mechanics of NAnofluids) experimental facility has been designed to allow the experimental comparison of the different behavior of nanofluids and base fluids (without nanoparticles), using two parallel identical loops. The facility allows to test the differences both in the heat transfer properties and in the mechanical effects on metal targets (erosion, corrosion etc.); the present paper will focus on the heat transfer issue. An additional special feature of the dual loop is the possibility to monitor in real time the difference in the heat transfer rate, thus allowing also to adjust the experimental test matrix during the test, on the basis of the results of previous tests. The precision is thus higher, because the control system keeps the two loops under identical conditions, and so little variations during the long-term tests can be considered negligible for the comparison.

3.1 Description of the Experimental Loop

A diagram of one of the two loops is shown in Fig. 1. The flow rate is controlled by a volumetric gear pump, and the flow-rate is

measured with a Coriolis flow-meter and remotely controlled by a Labview program.
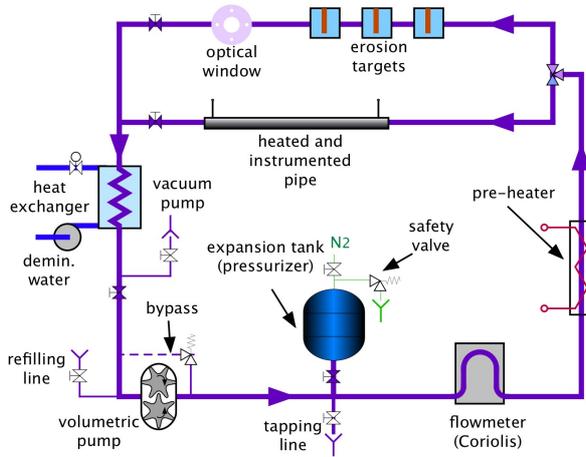
Fig. 1. Schematic of each of the two identical loops

The inlet temperature is controlled by a pre-heater and the pressure by an expansion tank.
The test section, shown in Fig. 2, is an AISI 316 pipe 4 mm ID, 0.25 mm in thickness and with a heated length of 200 mm. The wall temperature is measured by four thermocouples fixed on the external surface with a two components epossidic resin at the following distances from the inlet: 20, 73, 127, 180 mm. The pipe wall is thermally insulated and is heated by Joule effect with a DC power supply, and the test sections of the two loops are connected in series to have the same current and to obtain a total resistance ideal for the power supply.

Fig. 2. Test section without the thermal insulation

After the calibration tests with water, one of the loops is filled with the nanofluid. The heat transfer coefficient is calculated from the measured values of the wall and the fluid temperature in the heated pipe section. Tests are carried out at equal velocity, mass flow-rate or Reynolds number in the two loops, directly deriving the heat transfer ratio.
The ranges of the experimental conditions are:
  Specific Mass Flow-rate: 60 to 1600 kg/m^{2}s
  Velocity: 0.06 to 1.6 m/s

  Reynolds number: 100 to 12000
  Thermal power: 50 to 600 W
  Heat flux: 20 to 240 kW/m^2
  Inlet temperature: 20 to 65 °C
Most of the tests reported in the present work were carried out at fixed power (100 W), with varying flow-rate (an increase followed by a decrease to exclude any hysteresis effect), to obtain hundreds measurements over a wide range of velocity under quasi-steady conditions. The measurements are recorded every 20 s. Some other tests have been performed by changing the thermal power at a fixed flow-rate.

4. Data Reduction
The heat transfer coefficient corresponding to the four thermocouples is calculated starting from the measurement of the fluid inlet temperature, T_{fi}, and the external wall temperature, T_{we} (used to obtain T_{wi}), along with the delivered thermal power, W.
The inner wall temperature T_{wi} is derived from the external one using the Fourier's equation in cylindrical coordinates, under steady-state conditions and neglecting the axial conduction, but not the heat losses.
The heat losses through the insulation have been evaluated from the electric power necessary to keep the empty test section under steady conditions for different T_{we}.
Solving the equation

$$-\frac{q}{k} = \frac{1}{r}\frac{dT}{dr} + \frac{d^2T}{dr^2} \qquad (2)$$

with the boundary conditions

$$\begin{cases} T = T_{wi} & \big| \, r = R_i \\ \dfrac{dT}{dr} = \dfrac{W_{dis}}{k\,S_e} & \big| \, r = R_e \end{cases} \qquad (3)$$

we obtain

$$T_{wi} = T_{we} + \frac{1}{2\pi L k} \cdot$$
$$\cdot \left[\frac{W}{2} + \left(W_{dis} + \frac{W R_e^2}{R_e^2 - R_i^2} \right) \ln\left(\frac{R_e}{R_i} \right) \right] \qquad (4)$$

To evaluate the performance of the whole test section the average heat transfer coefficient will be used, given by:

$$h_{avg} = \left[h(x_1) + h(x_2) + h(x_3) + h(x_4) \right]/4 \qquad (5)$$

5. Experimental Results

The fluid condition in the heated test section is hydrodynamically developed but with the thermal entrance effect covering most of the test channel. Upstream of the channel inlet there is a calming length of 1 m (250 D with, however, a small disturbance induced by the 0.5 mm inlet thermocouple) while the minimum thermal entrance length for fully developed flow, generally obtained when Gz < 10, i.e., x* > 0.1, is never reached during the tests, as shown in the first tests [13].

The simple comparison of the experimental heat transfer coefficients of nanofluid and base fluid can lead up to very different conclusions depending on the parameter selected, as already noticed in [14, 15]: nanofluids provide higher value of thermal enhancement in higher Reynolds number, but in practical applications the increase should be compared in the same pumping power or the same mass flow rate. If the Reynolds number is used as shown in Fig. 3a, where the average heat transfer rate is plotted versus Re for both laminar and turbulent flow, the heat transfer coefficient enhancement for all nanofluids is mostly observed. These results might be also affected by the increase in the viscosity (greater than the density one, as seen in Table 1) and consequently by the higher mass flow-rate needed to have the same Reynolds number. On the other hand using the fluid velocity as a reference parameter, the behavior is completely different (Fig. 3b), where the average heat transfer rate is plotted versus the fluid velocity: the heat transfer coefficient for all nanofluids is mostly lower than that of water at the same velocity. In the very limited cases where it is higher than water, generally in laminar flow, the enhancement is negligible. In Fig. 4, the ratio between the heat transfer coefficients of the nanofluid (h_N) and water (h_W) is plotted, versus u (Fig. 4a) and Re (Fig. 4b) respectively.

The data refer to TiO_2-9wt% and to three solutions at different concentration of SiC, at a thermal input of 100 W (heat flux 40 kW/m^2), at the same time in the two loops (one with water and the other with the nanofluid), in the correspondence of the fourth thermocouple,

close to the exit (x=180 mm) of the test section.
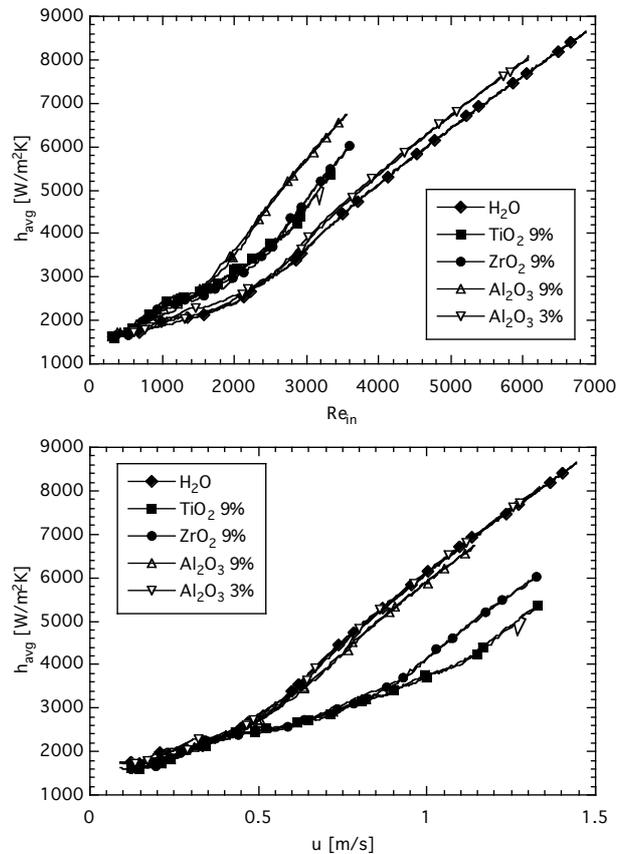
Fig. 3. Average heat transfer coefficient. Each curve represents about 400 experimental points - a) plotted vs. Reynolds number; b) vs. fluid velocity.

In the first case (Fig. 4a), except for very low fluid velocity, nanofluids thermal performance is generally smaller or not much better than water. In the second case, the thermal behavior of the nanofluids looks generally better than that of water for almost the whole range of Re. The significant reduction of the ratio h_N/h_W in the intermediate region of velocity is due to the different velocities at which the laminar to turbulent flow transition occurs in the nanofluid and in water. Since at fixed velocity, the nanofluid has a lower Reynolds number with respect to water, due to the higher viscosity, the laminar to turbulent flow transition for the nanofluid is *delayed* as much as the viscosity is higher than the base fluid.

Based on these considerations, the experimental data of the nanofluids not shown in the previous figures are reported as a function of velocity, only.

In Fig. 5 the heat transfer coefficients ratio is reported for water based nanofluids containing TiO_2, ZrO_2 or Al_2O_3 nanoparticles, close to the inlet (x=20 mm) and the exit (x=180 mm) of the test section.

The Al_2O_3 nanofluids exhibit the best performance , with a behavior similar to the Sic-3wt% shown in Fig. 4a.
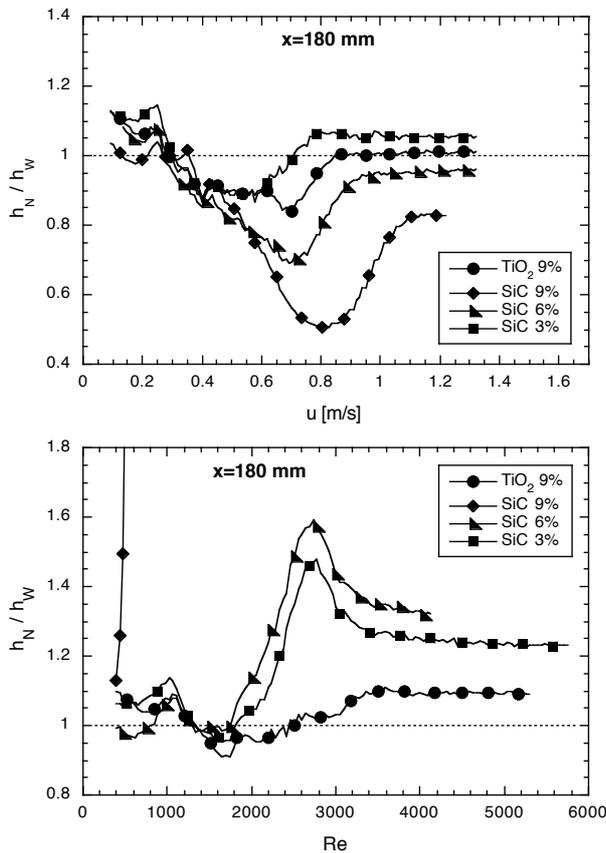
Fig. 4. Heat transfer coefficient ratio at position x_4, (close to test section exit) - a) plotted vs. fluid velocity; b) vs. Reynolds number.

Regarding the water-glycol based nanofluids, the results are reported in Fig. 6, where is shown the comparison between Al_2O_3-20wt% and Al_2O_3-9wt% and the relative base fluids, water/ethylene glycol (50% each) and water/Antifrogen-N (50% each), respectively. It is evident that a greater fraction of nanoparticles leads to an increase of the heat exchange. Considering the higher viscosity of the base fluids, with respect to water, the latter cases refer to laminar flow conditions, and so they should be compared with the results shown in Fig. 5b for velocity u<0.4 m/s, only. Even in this latter case, the increase in solids

content (from 3wt% to 9wt% Al_2O_3) involves an increase in the heat transfer coefficient.
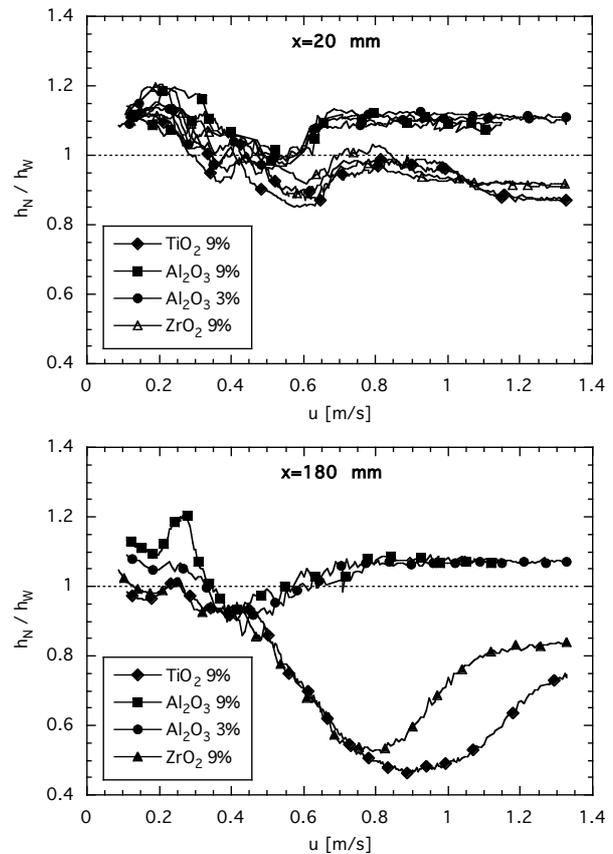
Fig. 5. Heat transfer coefficient ratio vs. fluid velocity at two positions

6. Data Analysis

The analysis of the experimental data, indicates that nanofluids' heat transfer coefficient does not seem to have a dramatic increase with respect to the corresponding base fluids, and differences appear to be associated to different flow conditions only. A confirmation of this result can be given by the comparison of nanofluids heat transfer coefficient with the predictions obtained using correlations originally developed for pure fluids. As far as these correlations account for actual fluid physical properties, predictions for water and nanofluid are similarly good, and thus we might conclude that the nanofluid can be regarded as a homogeneous mixture.

Therefore, its advantage with respect to classical coolants should be evaluated on the basis of its physical properties (μ, ρ, k, c_p). Since in the present experiments the Reynolds number ranged between 100 and 12000, more than one correlations for the evaluation of the

heat transfer coefficient (in terms of Nusselt number) had to be used (see Table 2).Furthermore, since for many experimental data the thermal entrance effect is present, those correlations have to take in account not fully developed conditions also.
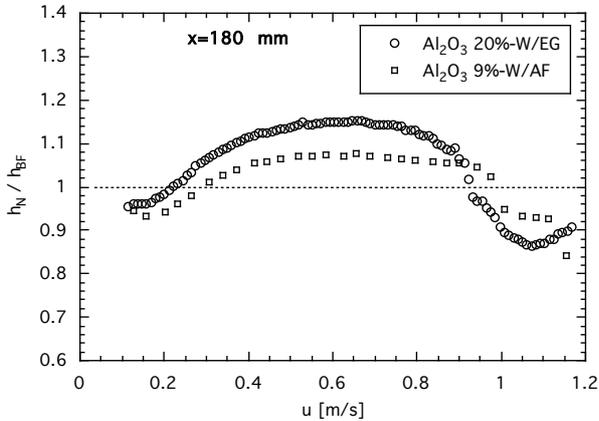
Fig. 6. Ratio between nanofluids and their base fluids heat transfer coefficient vs. fluid velocity for the water/glycol based nanofluids

The analyzed experimental data have been obtained testing 12 nanofluids and 3 base fluids, typically with W=100W and T_i=25°C. Some nanofluids have been tested also with different powers and inlet temperatures (23 tests have been made). Each test is result hundreds of experimental points obtained in a wide speed range, Fig.7.
The comparison of the experimental data with the available correlations has been carried out calculating the Root Mean Square Prediction Error, RMS, and Mean Relative Error, MRE, defined as follows:

$$MRE = \left(\sum_{1}^{n} \left(y_{cal} - y_{exp} \right) \middle/ y_{exp} \right) \middle/ n \qquad (6)$$

Table 2 shows the above parameters separately for water and nanofluids in laminar and turbulent flow.

6.1 Laminar flow
Correlations for laminar flow were compared with experimental data for *Re*<2500. From Table 2 it can be seen that in the case of laminar flow the best correlations are the Baehr-Stephan [15] and the Oskay-Kakac [14], (Table 3).
The first one provides average values higher than the experimental ones (*ME*>0 for both

water and nanofluids), while the second one provides basically underestimated values (*ME*<0).

Table 2
Mean error of the correlations

Author	Water		Nanofluids	
	RMS	MRE	RMS	MRE
Laminar flow	3889 points		13923 points	
Shah [16]	0.32	0.32	0.29	0.28
Baehr-Stephan [17]	0.20	0.18	0.17	0.13
Oskay-Kakac [16]	0.18	-0.07	0.20	-0.12
Stephan-Preuber [12]	0.29	-0.22	0.30	-0.25
Hausen [18]	0.26	0.24	0.23	0.20
Turbulent flow	6479 points		9861 points	
Colburn [16]	0.18	0.02	0.19	0.02
Hausen [16]	0.08	0.01	0.17	0.11
Sieder-Tate [16]	0.20	-0.02	0.21	-0.02
Gnielinski [16]	0.12	0.07	0.18	0.12
Gnielinski [19]	0.12	-0.07	0.14	-0.01

Fig. 7a shows the ratio Nu_{cal}/Nu_{exp} for the Baehr-Stephan correlation. For water-based nanofluids the Baehr-Stephan correlation underestimates the values of Nusselt number, in particular in the case of Al_2O_3-9% and *Re*>1500. The others fluids follow the trend of water, but generally with a smaller underestimation. Similar trends are obtained for the Oskay-Kakac correlation.

6.2 Turbulent flow
From Table 2 it can be seen that, for turbulent conditions, the best correlations are the Hausen [16] and Gnielinski [19], Table 3.
Fig. 7b shows the Nu_{cal}/Nu_{exp} ratio for the Gnielinski correlation. The worst prediction (marked underestimation) is associated with the Al_2O_3-9wt% nanofluid, despite its good experimental behavior: it can be observed that in this case the experimental heat transfer capability enhancement is larger than that expected by simply introducing the average physical properties of the fluid in the above correlations. The heat transfer efficiency of all the other nanofluids is predicted with a rather higher accuracy, showing a good agreement with the behavior expected from a homogeneous liquid with same physical properties. The Gnielinski correlation (10) gives better predictions for SiC and ZrO_2 nanofluids.

Table 3
Heat transfer correlations

Ref.	Correlation	Eq.
Baehr-Stephan [17]	$Nu = \dfrac{3.657}{\tanh\left(2.264\, x^{*(1/3)} + 1.7\, x^{*(2/3)}\right)} + \dfrac{0.0499}{x^*}\tanh x^*$	(7)
Oskay-Kakac [16]	$Nu = 1.86\, x^{*(-1/3)}\left(\mu/\mu_w\right)^{0.152}$	(8)
Hausen [16]	$Nu = 0.116\left(Re^{2/3} - 125\right) Pr^{1/3}\left[1 + \left(D/x\right)^{2/3}\right]\left(\mu/\mu_w\right)^{0.14}$	(9)
Gnielinski [19]	$Nu = \dfrac{f_1}{2}\dfrac{Pr\left(Re - 1000\right)}{1 + 12.7\sqrt{f_1/2}\left(Pr^{2/3} - 1\right)}\left[1 + \left(\dfrac{D}{x}\right)^{2/3}\right]$	(10)

Conclusions

The presented results show that the evaluation of the heat transfer performance of a nanofluid depends on the parameter adopted for the comparison. If the fluid velocity is used, the nanofluid heat transfer coefficient is generally lower than that of the basic fluid. Using the Reynolds number, the nanofluid heat transfer coefficient turns out to be higher than for the basic fluid. This is generally due to the higher viscosity of the nanofluid (the presence of nanoparticles increases the fluid viscosity with respect to the basic fluid) which for the same Reynolds number calls for a higher velocity (being the increase in the nanofluid density much smaller than in the viscosity), thus allowing a better heat transfer performance.

From the comparison with the classical literature correlations,it can be observed that the nanofluids containing Al_2O_3 particles show an experimental enhancement of heat transfer greater than expected, and this enhancement increases with the concentration of nanoparticles. For the other nanofluids the trend of the Nu_{cal}/Nu_{exp} is similar to that of water, so that most of the nanofluids behave like a homogeneous fluid with physical properties properly accounting for the presence of nanoparticles. Therefore, in these cases the possible heat transfer enhancement using nanofluids are still associated with the parameters commonly affecting the convective heat transfer mechanism (k, ρ, μ, c_p), which in the case of nanofluids also dependon the type, size, shape and volume of nanoparticle as well as on the possible presence of surfactants used to stabilize the nanofluid itself.
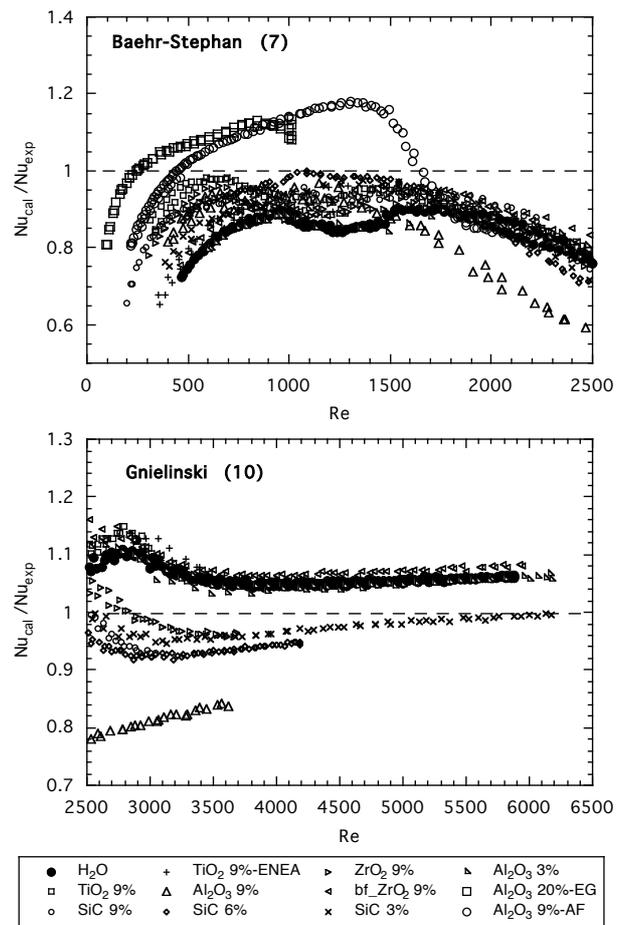
Fig. 7. Calculated on experimental Nusselt ratio: a) laminar conditions, for the equation (7) ; b) turbulent conditions, for the equation (10)

Nomenclature

AF   Antifrogen N
EG   Ethylene glycol
c_p specific heat [J/kg K]
D   diameter [m]

f_l Fanning friction factor[dimensionless]

Gz   Graetz number $Gz = D\,Re\,Pr/x$

h   heat transfer coefficient [W/m^{2}K]

k   thermal conductivity [W/m K]

L   test section length [m]

Nu   Nusselt number [dimensionless]

Pr   Prandtl number [dimensionless]

q   heat flux [W/m^2]

r   radial coordinate [m]

R   test section radius [m]

Re   Reynolds number [dimensionless]

S   surface [m^2]

T   temperature [°C]

wt   fraction in weight

W   thermal power [W]

x   distance from the inlet [m]

x*   non-dimensional axial length 1/Gz

Greek Symbols

μ   viscosity [N s/m^2]

ρ   density [kg/m^3]

Φ_{vol} particle volume concentration

$$\phi_{vol} = \phi/\left(\phi + (1-\phi)\rho_P/\rho_{BF}\right)$$

Subscripts

avg   average

BF   base fluid

cal   calculated

dis   dispersed

e   external

Exp   experimental

f   fluid

i   internal

N   nanofluid

P   particle

w   wall

W   water

x   relative to the position x

References

[1] Saidur, R., Leong, K.Y., Mohammed, H.A., A review on applications and challenges of nanofluids, *Renew. Sust. Energ. Rev.*, Vol. 15, pp. 1646-1648, 2011.

[2] Das, S.K., Choi, S.U.S., and Patel, H.E., Heat Transfer in Nanofluids-A Review, *Heat Transfer Eng.*, Vol. 27, pp. 3-19, 2006.

[3] Das, S.K., Choi, S.U.S., Yu, W., and Pradeep, T., Nanofluids Science and Technology, *John Wiley & Sons, Inc.*, Hoboken, NJ, 2008.

[4] Lee, J., and Mudawar, I., Assessment of the effectiveness of nanofluids for single-phase and two-phase heat transfer in micro-channels, *International Journal of Heat and Mass Transfer*, Vol. 50, pp. 452-463, 2007.

[5] Yu, W., France, D.M., Routbort, J.L., andChoi, S.U.S., Review and Comparison of Nanofluid Thermal Conductivity and Heat Transfer Enhancements, *Heat Transfer Eng.*, Vol. 29, pp. 432-460, 2008.

[6] Cheng, L., Bandarra Filho, E.P., and Thome, J.R.: Nanofluid Two-Phase Flow and Thermal Physics: A New Research Frontier of Nanotechnology and Its Challenges. *J. Nanosci. Nanotech.*, Vol. 8, pp. 3315-3332, 2008.

[7] Wen, D., and Ding, Y., Experimental investigation into convective heat transfer of nanofluids at the entrance region under laminar flow conditions, *Int. J. Heat Mass Transfer*, Vol. 47, 2004.

[8] Maré, T., Halelfadl, S., Sow, O., Estellé, P., Duret, S., Bazantay, F., Comparison of the thermal performances of two nanofluids at low temperature in a plate heat exchanger, *Experimental Thermal and Fluid Science*, Vol. 35, pp. 1535–1543, 2011

[9] Duangthongsuk, W., and Wongwises, S., An experimental study on the heat transfer performance and pressure drop of TiO2-water nanofluids flowing under turbulent flow regime, *International Journal of Heat and Mass Transfer*, Vol. 53, pp. 334-344, 2010

[10] Pak, B.C., Cho, Y.I., Hydrodynamic and Heat Transfer Study af Dispersed Fluids with Submicron Metallic Oxide Particles, *Experimental Heat Transfer*, Vol. 11, pp. 151-170, 1998

[11] Williams, W., Buongiorno, J., and Hu, L.W., Experimental investigation of turbulent convective heat transfer and pressure loss of alumina/water and zirconia/water nanoparticle colloids (nanofluids) in horizontal tubes, *J. Heat Transfer*, Vol. 130, p. 042412, 2008.

[12] Liu, D., Yu, L., Single-Phase Thermal Transport of Nanofluids in a Minichannel, *J. Heat Transfer,* Vol. 133, p. 031009, 2011

[13] Celata, G.P., D'Annibale, F., Mariani, A., Saraceno, L., D'Amato, R., Bubbico, R., Heat Transfer in Water-Based SiC and TiO2 Nanofluids, *Heat Transfer Engineering*, 34(13):1060–1072, 2013

[14] Bayat J., Nikseresht A.H. International Journal of Thermal Sciences 60 236-243, 2012.

[15] Yu W., France D. M.,. Timofeeva E. V, Singh D. and.Routbort J.L .Thermophysical property-related comparison criteria for nanofluid heat transfer enhancement in turbolent flow. Applied physics letters 96, 213109 ,2010.

[16] Kakac, S., Shah, R.K., Aung, W., Handbook of Single-Phase Convective Heat Transfer, *Wiley*, New York, 1987.

[17] Stephan, P., Fundamentals of Heat Transfer, in: VDI Heat Atlas 2th Edition, *Springer*, 2010.

[18] Thirumaleshwar, M., Fundamentals of Heat & Mass Transfer, *Pearson Education*, p. 453, 2006

[19] Gnielinski, V., Forced Convection in Ducts, in: G.F. Hewitt (Ed.), Heat ExchangerDesign Handbook, Begell House Inc., New York, 1998.